LAWRENCE
LIVERMORE
NATIONAL
LABORATORY

UCRL-JRNL-216587

A NON-CLEAVABLE UmuD VARIANT THAT ACTS AS A UmuD' MIMIC

P. J. Beuning, S. M. Simon, A. Zemla, D. Barsky, G. C. Walker

October 27, 2005

Journal of Biological Chemistry

A NON-CLEAVABLE UmuD VARIANT THAT ACTS AS A UmuD' MIMIC

Penny J. Beuning[1], Sharotka M. Simon[1], Adam Zemla[2], Daniel Barsky[3], and Graham C. Walker[1]

[1]Department of Biology, Massachusetts Institute of Technology, Cambridge, MA 02139
[2]Computations Directorate and [3]Biosciences Directorate, Lawrence Livermore National Laboratory, Livermore, CA 94550

Address correspondence to: Graham C. Walker, Massachusetts Institute of Technology, Department of Biology, 68-633, 77 Massachusetts Ave, Cambridge, MA 02139, Phone: 617-253-6716, Fax: 617-253-2643, Email: gwalker@mit.edu

$UmuD_2$ cleaves and removes its N-terminal 24 amino acids to form $UmuD'_2$, which activates UmuC for its role in UV-induced mutagenesis in *E. coli*. Cells with a non-cleavable UmuD exhibit essentially no UV-induced mutagenesis and are hypersensitive to killing by UV light. UmuD has been shown to bind to the beta processivity clamp ("beta") of the replicative DNA polymerase, pol III. A possible beta-binding motif has been predicted in the same region of UmuD shown to be important for its interaction with beta. We performed alanine-scanning mutagenesis of this motif (14-TFPLF-18) in UmuD and showed that it has a moderate influence on UV-induced mutagenesis but is required for the cold sensitive phenotype caused by elevated levels of wild-type UmuD and UmuC. Surprisingly, the wild-type and the beta-binding motif variant bind to beta with similar K_d values as determined by changes in tryptophan fluorescence. However, this data also implies that the single tryptophan in beta is in strikingly different environments in the presence of the wild-type versus the variant UmuD proteins, suggesting a distinct change in some aspect of the interaction with little change in its strength. Despite the fact that this novel UmuD variant is non-cleavable, we find that cells harboring it exhibit phenotypes more consistent with the cleaved form UmuD', such as resistance to killing by UV light and failure to exhibit the cold sensitive phenotype. Cross-linking and chemical modification experiments indicate that the N-terminal arms of the UmuD variant are less likely to be bound to the globular domain than those of the wild-type, which may be the mechanism by which this UmuD variant acts as a UmuD' mimic.

The *umuDC* gene products are induced as part of the SOS response and are responsible for much of the UV-induced mutagenesis in *E. coli* (1). These gene products are subject to an elaborate set of controls that regulate their activity (1). The LexA repressor provides transcriptional control, and there are several proteolytic controls on both the *umuD* and *umuC* gene products (1). The homodimeric protein $UmuD_2$ is the predominant species during the first ca. 20-30 min after SOS induction (2). $UmuD_2$, together with UmuC, plays a role in a DNA damage checkpoint, decreasing the rate of DNA synthesis and allowing time for accurate repair processes to act (2). This correlates with the cold sensitive phenotype observed under conditions of overexpression of the *umuDC* gene products (2,3). As the SOS response proceeds, $UmuD_2$ binds the RecA/ssDNA nucleoprotein filament. This stimulates the latent ability of $UmuD_2$ to convert to $UmuD'_2$ by cleaving off its N-terminal 24 amino acids, resulting in $UmuD'_2$ becoming the predominant species. The RecA/ssDNA nucleoprotein filament serves to

bring together the active site dyad residues Ser60 and Lys97, facilitating deprotonation of Ser60 by Lys97 (4). The activated Ser nucleophile then cleaves the peptide bond between Cys24 and Gly25 of $UmuD_2$ (1).

The wealth of structural data and models available for $UmuD_2$ and $UmuD'_2$ provide insight into how the two forms of the *umuD* gene products engage in multiple highly specific interactions (Fig. 1) (4-7), including with the α, β, and ε subunits of the replicative polymerase, pol III (8). Of the two forms, $UmuD_2$ interacts more strongly with the β processivity clamp (also referred to as β or the β clamp) than does $UmuD'_2$ (8,9). In full-length $UmuD_2$, the 39-amino acid N-terminal arms are stably bound to the globular C-terminal domain (4,7) and form a distinct interaction surface. In the cleaved form of the protein, $UmuD'_2$, the remaining ca. 15 amino acids at the N-terminus appear unbound from the body of the protein and solvent-exposed (5,6), revealing the buried portion of the C-terminal globular domain (4,7). A series of truncations at the N-terminal arm of $UmuD_2$ indicates that the first eight amino acids of $UmuD_2$ are dispensable for the $UmuD_2$-β interaction, while deleting residues 2-18 results in a substantial decrease in, but not a complete loss of, cross-linking efficiency with the β clamp (9). Thus, the *umuD* gene products interact with the β clamp via both the N-terminal arms of $UmuD_2$ and the globular domain of $UmuD_2$ and $UmuD'_2$ (9). This differential interaction appears to control, at least in part, whether the *umuDC* gene products act as part of a DNA damage checkpoint or as a translesion polymerase (8,9). These interactions with the β clamp are of particular interest since sliding clamps play a key role in coordinating the multiple DNA polymerases present in cells (10-14). The eukaryotic DNA sliding clamp PCNA interacts with multiple proteins, and these interactions are in part regulated by covalent modification of PCNA with monoubiquitin or the small ubiquitin-like modifier (SUMO) (15-18). Duzen *et al* have suggested that $UmuD_2$ and $UmuD'_2$ play conceptually similar roles in modulating the various clamp interactions (19).

A version of the canonical β clamp binding motif found in eubacterial polymerases as well as other proteins involved in DNA metabolism was postulated to be present in UmuD at residues 14-18 (Fig. 1) (20). A yeast two-hybrid experiment with the motif of UmuD showed, however, that these five amino acids are not sufficient for the interaction with the β clamp (20). Given the fact that this result was obtained utilizing only the five-amino acid motif in UmuD, and cross-linking experiments showed that the region of UmuD between residues 9 and 19 is important for interactions with the β clamp (9), we undertook a site-directed mutagenesis analysis of this motif. These studies led to the unexpected discovery of a new class of UmuD variant proteins that fail to undergo cleavage but whose properties resemble those of the cleaved version, UmuD'.

MATERIALS AND METHODS

Homology Model of UmuD- The models of the UmuD homodimer were created by the combined use of the program LGA (21) for protein structure comparison and superposition and the AS2TS program (22) for homology model-building. An initial model of the UmuD monomer (single chain) was constructed based on the crystal structure of UmuD' (Protein Data Bank [www.pdb.org] ID: 1ay9, chain A) (23). The missing N-terminal arm was modeled by the LGA loop building/grafting procedure (21), using mainly the arm conformation in 1jhh_A, from the X-ray crystallographic structure of LexA (24) as well as the other LexA structures (1jhc, 1jhe, 1jhf) as template structures to guide the local and overall conformation. In the final alignment (Fig. S1), UmuD Asp20 had to be inserted into the LexA template (between

residues 80 and 81 of LexA) and this was done by the LGA loop building procedure (21). Finally, residues 1-14 are in an extended conformation (i.e., we make no prediction as to the placement of these residues; they are only modeled in a formal sense).

In creating the full UmuD homodimeric complex, we used LGA to superimpose our monomer model onto each of the template chains in the NMR structure of the UmuD' homodimer (4) (1i4v, chains A and B, model #1), but some minor clashes occurred which were alleviated by following the LexA homodimer instead (24). This procedure creates a cis (non-domain swapped) conformation of the UmuD homodimer. Because there is a very small "shoulder" region at the top of the arms, the trans UmuD homodimer model could be constructed from the cis UmuD homodimer model by swapping the arms as follows: the first 39 residues in the chain A of our trans model were taken from the chain B of the cis model, and vice versa. This process of "arm swapping" was completed after applying the LGA loop building procedure to residues 39-41 in the shoulder regions. Finally, the LexA structures appear as both "elbows up" (N-terminal arm unbound) and "elbows down" (N-terminal arm bound to C-terminal domain), allowing us to model both conformations (Fig. S1). Thus, we created four models, two cis and two trans, each with an elbows up and an elbows down conformation. (It is possible that heterogeneous conformations also occur with one elbow up and one elbow down as in the 1jhh LexA structure.) For all the cis and trans models of the UmuD homodimer, the conformations of sidechains from residues either not present in 1ay9_A or that presented a steric clash after building the dimeric structures were modeled using the side-chain placement program SCWRL (25).

Proteins, Strains and Plasmids- A plasmid expressing UmuD-3A was constructed in pSG5 using mutagenic primers and the Quikchange kit (Stratagene). Wild-type UmuD and UmuD-3A were purified according to the published procedure (26). The plasmid expressing His-HMK-β was a gift from M. O'Donnell (Rockefeller University), and β was purified according to the published procedure (27). All primer sequences are available upon request. The strains and plasmids used in this study are listed in Table 1. Plasmid pSJS9 was a gift from Prof. Charles McHenry (Univ. Colorado). Site-directed mutagenesis was performed using the Quikchange kit (Stratagene).

Mutagenesis and Survival Assays- SOS mutagenesis assays were performed according to the published method (26). Briefly, cultures of GW8017 harboring various *umuDC*-expressing plasmids growing exponentially in LB were washed with 0.85% saline, exposed to 25 J/m^2 UV light from a germicidal lamp (General Electric), and then plated on M9 minimal plates with trace arginine (1 μg/mL). Colony-forming units were scored after 48 hr of growth at 42 ºC. Survival was determined by plating on M9 minimal plates with 40 μg/mL arginine. Non-UV irradiated cultures were treated identically to assess the spontaneous mutation frequency. The data represent the average of at least three independent experiments.

UV survival curves were obtained after treating cells in a Petri dish with the indicated doses of 254-nm light. Each sample was serially diluted and the dilutions plated on M9 minimal media plates supplemented with 1% casamino acids, 0.005% tryptophan, and 1.5% agar. Plates were incubated overnight at 42 °C.

Quantitative Transformation Assays- Transformation assays were performed essentially as described (26). Plasmids (0.1 μg) were added to 25 μL competent AB1157 cells and incubated on ice for 10 min. After a 5-min heat shock at 37 ºC, and a further 10-min incubation on ice, transformation

mixtures were allowed to recover in 750 µL LB at 37 ºC for 1.5 hr with gentle shaking. Equal volumes were plated on LB plates containing the appropriate antibiotics for incubation under different temperatures as indicated in the figure legends.

Immunoblots- To determine UmuD expression levels, cells were harvested from exponentially growing cultures in LB, lysed by boiling for 15 min, and loaded on 4-20% SDS-polyacrylamide gradient gels (Cambrex). Electrophoresed proteins were transferred to PVDF membrane (Millipore) in 10 mM CAPS, pH 8, 10% methanol. After blocking, membranes were probed with anti-UmuD/D', and antibody interactions were detected with SuperSignal substrate (Pierce). For UV-induced expression and cleavage experiments, an aliquot of ca. 2.5 x 10^{10} cells from an exponentially growing culture at OD_{600} = 0.2-0.3 was harvested, washed in 0.85% saline and UV-irradiated at 25 J/m^2. Irradiated cells were then transferred to LB and grown at 37 ºC for the times indicated in the figure legend.

UmuD in vitro *Cleavage Assay*- RecA/ssDNA nucleoprotein filament-facilitated UmuD cleavage was assayed (26,28,29) in LG buffer for 30 min. Reactions were quenched by addition of SDS-PAGE buffer to 1x, and products were analyzed on 4-12% gradient polyacrylamide gels. Alkaline cleavage of UmuD was carried out (26,30) in 100 mM glycine, pH 10, 10 mM $CaCl_2$, 50 mM NaCl, 10 mM DTT, and 0.25 µg/mL BSA for 48 hr at 37 °C. Reaction products were analyzed by 14% polyacrylamide gel electrophoresis.

Cross-linking and Chemical Modification- Cross-linking was performed essentially as described (31) with bis-maleimidohexane (BMH, Pierce). Reactions were incubated at room temperature for the times indicated. For chemical modification with 5,5'-dithiobis(2-nitrobenzoate) (DTNB) (32), DTNB was dissolved at 2 mM final concentration in 50 mM HEPES, pH 7.5. Reactions were performed with 10-20 µM DTNB and 10-20 µM UmuD proteins in 50 mM HEPES, pH 7.5. The concentration of accessible thiols was calculated with an extinction coefficient of 13600 cm^{-1} M^{-1} at 412 nm. Several trials were performed, and representative data is shown.

Fluorescence Determination of Binding Constants- Binding constants between UmuD and β were determined essentially as described, with a PT1 QM-20000-4SE spectrofluorimeter (Lawrenceville, NJ) (26). The β clamp has a single Trp (residue 122), while UmuD has none. The β_2 concentration was constant at 2.5 µM. Emission from UmuD or UmuD-3A without β_2 was subtracted from emission of the complex, and the center of spectral mass was calculated for each [UmuD]. Excitation was at 278 nm, and emission was monitored from 300 to 400 nm. Excitation and emission path polarizers were oriented perpendicularly. The data represent the average of at least three independent experiments ± one standard deviation.

RESULTS

Mutations in "b-binding motif" of UmuD do not result in complete loss of induced mutagenesis- We used alanine-scanning mutagenesis to make single alanine mutations in the putative β-binding motif in UmuD (Fig. 1 and Fig. 2) and investigated the consequences of these variants on known phenotypes of UmuD. These plasmid-borne variants were assayed for their ability to complement a Δ*umuDC* null strain for UV-induced mutagenesis. In addition to single alanine variants of UmuD, we constructed one variant with alanines at the first and last two positions in the motif (UmuD-3A, Fig. 2), the positions most conserved among all β-binding motifs (20). In the case of UmuC, the analogous mutation in its β-binding motif results in a complete loss of UV-induced mutagenesis (10,11). No single mutation or set

of multiple mutations in this motif in UmuD failed completely to complement a Δ*umuDC* strain. However, plasmids expressing either the F18A UmuD variant, which is located at the top of the arm over the C-terminal globular domain, or the T14A L17A F18A ("UmuD-3A") variant resulted in substantial decreases in induced mutagenesis, down to about 5% of the wild-type (Fig. 2). Curiously, this decrease in mutagenesis of cells harboring these variants was not accompanied by a corresponding decrease in survival after UV irradiation; yet, typically, increased mutagenesis due to translesion synthesis by UmuD'$_2$C is associated with increased survival after treatment with UV.

Cleavage of the N-terminal 24 amino acids from the arm of UmuD to yield UmuD' is required to activate UmuC for its role in translesion synthesis (1). Since the UmuD arm harboring these mutations would be removed upon cleavage, we reasoned that the defect in induced mutagenesis of strains expressing the F18A and T14A L17A F18A (UmuD-3A) variant proteins might be due to defects in cleavage. Given their positions in the N-terminal arm (Fig. 1), it might be expected that these residues would play a role in properly positioning the arm in the active site for cleavage. We tested whether these mutations in the N-terminal arm of UmuD interfered with cleavage after UV-exposure. The F15A mutant showed a slight decrease in cleavage and an approximately two-fold decrease in induced mutagenesis compared to the wild-type (Fig. 3). The two UmuD variants (F18A and UmuD-3A) that showed essentially no cleavage up to 3 h after UV exposure (Fig. 3), or even after 14 h (data not shown), resulted in the greatest reduction in induced mutagenesis (ca. 20% of wild-type). This is in contrast to non-cleavable active site UmuD variants that have been assayed previously, which showed essentially complete loss of induced mutagenesis (the limit of detection of this assay is ca. 1000-fold, or 0.1% of wild-type) (33,34). Thus, there are two groups of non-cleavable UmuD variants, one of which renders cells partially mutable and the other that renders cells completely non-mutable.

The wild-type and UmuD-3A variant proteins were purified in order to assess their efficiency in *in vitro* cleavage facilitated by the RecA/ssDNA nucleoprotein filament. Under these conditions, UmuD$_2$ is cleaved efficiently to form UmuD'$_2$, while UmuD-3A$_2$ exhibits no detectable cleavage (Fig. 3). Here again, the lack of cleavage is similar to that exhibited by the active site mutant of UmuD$_2$, UmuD-S60A$_2$ (33). We note that there is a lower band present in some of the samples incubated *without* the RecA/ssDNA nucleoprotein filament. This lower band is often observed in preparations of UmuD, and even in some preparations of UmuD-S60A. However, in the case of UmuD-3A, the intensity of the lower band does not increase after incubation with the RecA/ssDNA nucleoprotein filament.

UmuD forms exchangeable dimers (33), so wild-type UmuD$_2$ was combined with UmuD-3A$_2$, and cleavage was observed (Fig. 3). Since UmuD-3A cannot cleave its own arm, the observed cleavage is likely due to the active site catalytic dyad of UmuD-3A acting on the wild-type partner's arm, although the reverse is also possible. In this experiment it is also possible that the cleavage observed is due entirely to a small population of wild-type UmuD$_2$ homodimers. To eliminate this possibility, UmuD-3A$_2$ was incubated with the active site variant UmuD-S60A$_2$, and some cleavage was still detected (Fig. 3). This slight cleavage must be due to the active site residues of UmuD-3A cleaving the arm of UmuD-S60A, which suggests that the active site of UmuD-3A is proficient for cleavage and that the cleavage defect is isolated to its arm. The mutations in UmuD-3A at the top of the arm may disrupt folding of the arm over the globular domain or may interfere with

specific protein-protein contacts required to facilitate cleavage (Fig. 1).

To ensure that the cleavage defect was not due to defective interactions of UmuD-$3A_2$ with the RecA/ssDNA nucleoprotein filament, we also carried out cleavage under alkaline conditions in the absence of the RecA/ssDNA nucleoprotein filament. The RecA/ssDNA nucleoprotein filament serves to facilitate deprotonation of Ser60 by a neutral Lys97 (4,24). In the absence of the RecA/ssDNA nucleoprotein filament, the activation of Ser60 as a nucleophile can be accomplished under alkaline conditions. Under these conditions, $UmuD_2$ cleavage is inefficient but can be detected (30). We found that cleavage of UmuD-$3A_2$ was substantially decreased compared to that of the wild-type (Fig. 3). This suggests that the cleavage defect of UmuD-$3A_2$ is due to a defect intrinsic to the UmuD-$3A_2$ variant rather than deficient interactions with the RecA/ssDNA filament.

UmuD-3A fails to exhibit the cold sensitive phenotype- Strains with elevated levels of the *umuDC* gene products exhibit a cold-sensitive phenotype that correlates with a DNA damage checkpoint (2,3). Cells harboring plasmids overexpressing the cleavable *umuD* variants T14A and F15A (+ wild-type *umuC*) were also cold sensitive. The T14A and F15A variants behave similarly to wild-type in terms of their ability to exert the cold sensitive phenotype, to be cleaved to UmuD', and to act in UV-induced mutagenesis. The cold sensitive phenotype is substantially enhanced in cells overexpressing the non-cleavable variant UmuD-S60A (Fig. 4) (35). Thus, we were surprised to find that strains harboring plasmids expressing the noncleavable *umuD* arm variants (UmuD-F18A and UmuD-3A) failed to display this cold-sensitive phenotype (Fig. 1 and Fig. 4).

We hypothesized that the loss of the cold sensitive phenotype was due to the specific arm mutations of UmuD, regardless of their cleavage defect. To test this, we combined in single constructs either the UmuD-F18A or UmuD-3A arm mutations with the S60A mutation that renders UmuD catalytically inactive. Even though they are not cleavable, the arm mutations F18A and UmuD-3A alleviated the extreme cold sensitivity exhibited by strains with elevated levels of UmuD-S60A (Fig. 4). Although strains harboring plasmids overexpressing the UmuD F18A S60A double mutant display a cold sensitive phenotype that is intermediate between that of cells with each corresponding single mutant, the cold sensitive phenotype of cells overexpressing UmuD-S60A is suppressed by two orders of magnitude by the presence of only a single mutation in the N-terminal arm, F18A. These arm variants must disrupt a specific molecular interaction necessary to cause the cold sensitive phenotype that is independent of whether they can be cleaved.

Simultaneously elevated levels of the *umuD*, *umuC*, and *dnaN* (which codes for the β clamp) gene products cause a lethal phenotype, which has been interpreted as an exaggeration of the cold sensitive phenotype (36). A strain harboring a plasmid expressing UmuD-3A and UmuC, when combined with high levels of the β clamp, fails to exhibit the synthetic lethal phenotype (Table 2). This suggests that a critical aspect of this complex formation with β is disrupted in the UmuD-3A variant.

Sensitivity to UV exposure- Given the cleavage defect of the UmuD-3A and F18A N-terminal arm variants, we decided to look more closely at the curious lack of a correlation between UV mutability and survival after exposure to UV that we had noted earlier for cells expressing the F18A and UmuD-3A variants. It is known that *E. coli* strains harboring a non-cleavable UmuD variant are hypersensitive to killing by UV light and are non-mutable (2,33) (Fig. 5). In order to determine whether this is also true of the non-cleavable UmuD F18A and UmuD-

3A variants, strains harboring plasmid-borne *umuD* variants were assayed for their resistance to UV light. Strains with plasmids expressing either of the non-cleavable variants F18A or UmuD-3A showed a similar level of resistance to UV light as those expressing wild-type UmuD or a synthetic construct of UmuD' (Fig. 5). We suspected that the resistance to killing by UV of the F18A and UmuD-3A variants was due to a specific feature of the arm mutants, unrelated to their cleavage defect. Cells with plasmids expressing the non-cleavable arm variants constructed in the context of the UmuD-S60A active site variant were assayed for their resistance to UV light. Strains with plasmids expressing either the F18A or UmuD-3A arm variants combined with UmuD-S60A exhibited a striking resistance to UV light that was similar to strains with wild-type UmuD (Fig. 5). This suggests that alterations in the N-terminal arm of UmuD are able to suppress the extreme UV-sensitive phenotype of non-cleavable UmuD-S60A, even though they are also non-cleavable. In light of the dramatic changes in the phenotypes of cells expressing the UmuD-3A variant compared to those with previously characterized non-cleavable variants of UmuD (33), we investigated the conformational consequences of the UmuD-3A variant compared to the wild-type.

Chemical cross-linking and modification of UmuD homodimers- We hypothesized that these non-cleavable UmuD variants are able to confer resistance to UV light, as well as to suppress the cold sensitive phenotype, by mimicking the conformation of UmuD'. To examine this possibility, we analyzed the conformation of the N-terminal arm of the UmuD-3A variant compared to the wild-type UmuD. UmuD, which possesses a C_2 axis of symmetry, has a single Cys residue, Cys24, at the cleavage site in the N-terminal arm. In order to determine whether UmuD-3A is a UmuD' mimic with respect to the position of its arms, cross-linking was performed with the thiol-specific homobifunctional 16 Å cross-linker bis-maleimidohexane (BMH). Our model allows us to put a lower limit of 20 Å on the distance between these two Cys thiols. This lower limit represents an implausible path for the cross-linker, since it is the direct distance between the two Cys thiols (Fig. 1). Thus, cross-linking should only be detected when the arms are "up", i.e. not bound to the C-terminal globular domain of UmuD. UmuD-3A was more readily cross-linked by BMH than either wild-type UmuD or UmuD-S60A (Fig. 6), suggesting that the arms of UmuD-3A are less likely to be bound to the globular domain of UmuD. Therefore they are more often close enough to be cross-linked.

One of the models of UmuD that we have proposed ("trans, elbows down", see Fig. 1 and Fig. S1) predicts that the thiol group of the single Cys24 residue is partially buried under the peptide backbone of the N-terminal arm. However, if the UmuD arms are in an "up", or more flexible, conformation, then the Cys should be more accessible to a thiol-specific reagent. We performed a titration of the Cys residue at the Cys24-Gly25 cleavage site with 5,5'-dithiobis(2-nitrobenzoate) (DTNB). The thiol moiety of UmuD-3A was more reactive to DTNB and therefore slightly more accessible than that of the wild-type UmuD (Fig. 6). We determined that there is 1.0 reactive Cys residue per wild-type $UmuD_2$ and 1.2 reactive Cys residues per $UmuD\text{-}3A_2$, supporting the idea that in the UmuD-3A variant, the N-terminal arms undergo a shift in equilibrium to a less bound, arms-up state.

Determination of K_d of UmuD and the β clamp- In order to quantify the binding of UmuD and the UmuD-3A variant to the β clamp, we determined the K_d for this interaction. Surprisingly, we found that although the K_d is similar for β binding to either wild-type UmuD (5.5 ± 0.8 μM) or UmuD-3A (6.1 ± 0.5 μM), the mode of binding is different for each protein. Namely,

the fluorescence emission from the tryptophan in β shifts to a longer wavelength upon binding to UmuD, while the shift is to a shorter wavelength in the presence of UmuD-3A (Fig. 7). Tryptophan fluorescence emission peaks at a longer wavelength in a polar environment and at a shorter wavelength in a hydrophobic one, indicating that the partially-exposed tryptophan in β (Fig. 1) becomes more solvent-exposed upon binding to wild-type UmuD and buried upon binding to UmuD-3A (37). Accordingly, unlike canonical β-binding motifs (10,11,38,39), this motif in UmuD is not responsible for the strength of the interaction with β, but rather for a qualitatively different mode of binding.

DISCUSSION

Although this work was initiated to determine the role of the putative β-binding motif (14-TFPLF-18) in UmuD function, we found that alterations in the motif do not prevent binding to the β clamp, unlike corresponding mutations in UmuC, DinB, and the pol III α subunit (10,11,20,38,39). Instead, we show here that the UmuD-3A variant alters the N-terminal arm conformation in a way that dramatically changes UmuD activity, and seems to exhibit properties of UmuD', particularly with respect to resistance to killing by exposure to UV light and lack of the cold sensitive phenotype when overexpressed together with UmuC. The UmuD-3A variant shows no defect in survival but decreases UV mutagenesis. This suggests that this variant may allow selective bypass of T:T cyclobutane pyrimidine dimers (CPDs) but not [6-4] photoproducts, since lethality is associated with T:T CPDs and mutagenesis with [6-4] photoproducts (1).

How could an uncleaved UmuD mimic the cleaved form, UmuD'? Current evidence suggests that the N-terminal arms of UmuD are usually bound to the C-terminal globular domain of the protein, i.e. it is usually in the "elbows down" conformation (7). Even when the arms are covalently bound to the globular domain, UmuD can be cross-linked to the β clamp with almost no decrease in efficiency (9). When UmuD is cleaved to UmuD', the remainder of the N-terminal arm (residues 25-39) is able to move relatively freely (5,23). The UmuD-3A variant seems to have enough flexibility in its arms that it is at least a partial mimic of UmuD'. Although residues 14-18 of UmuD are predicted from our model to be only partially buried (Fig. 1), the UmuD-3A variant may disrupt optimal packing of the arm against the globular domain. The mutations in UmuD-3A are at the point of the N-terminal arm that begins a downward turn over the C-terminal globular domain, and disruption of this turn is consistent with the more extended UmuD' arm structure. In addition, the cleavage of UmuD exposes a different surface of UmuD' for protein-protein interactions. Thus, the cleavage reaction serves the dual function of removing a portion of the N-terminal arms and presenting a dramatically different surface of the protein for interactions.

We were able to create models of the UmuD homodimer in both the elbows up and the elbows down conformation because both conformations are observed in the LexA structures (24). The LexA structure is in a cis conformation (not domain swapped) with respect to the positioning of the arms (24). We have noticed, however, that in the UmuD'$_2$ structures the truncated arms point in the trans direction, suggesting that perhaps the trans conformation is actually preferred for UmuD (5,6). It has been shown that UmuD can undergo cleavage in trans (Fig 3) (5,40). The model of UmuD most consistent with the available biochemical evidence is one in which the arms are in the trans conformation (7).

In constructing the UmuD-3A variant, we have made a version of UmuD that binds to the β clamp with a similar affinity as the wild-type, but with a subtle change in the

specific interaction as evidenced by the strikingly different tryptophan fluorescence emission spectra. This change would not have been detected by many of the techniques commonly used to detect protein-protein interactions, such as co-immunoprecipitation or two-hybrid analysis. Recent evidence suggests that the domains of the sliding clamps are rigid bodies joined by flexible linker regions (41). The single tryptophan of β is on a long flexible loop between rigid Domains I and II (Fig. 7) (42), so UmuD binding at a distal site to the tryptophan could cause a slight conformational rearrangement of the domains that alters the environment of the tryptophan in the loop. UmuD and DinB/pol IV bind to β at overlapping sites (Fig. 7) (19,43). One of these sites is the hydrophobic channel between β Domains II and III where all known β-binding motifs interact (43-45). Although UmuD possesses a similar motif to a canonical β-binding motif that modulates its interaction with the β clamp, and UmuD has been shown to bind to the same site on β as other β-binding motifs, it does so in a way that is distinct from other proteins that bind β via their β-binding motifs (45).

Processivity clamps play a critical role in controlling traffic at the replication fork and in cell cycle checkpoints. Polymerase binding to the β clamp regulates access to the primer terminus by replicative or translesion synthesis DNA polymerases (12,13). Moreover, it has been shown that UmuD interacts more strongly with β than UmuD' does (8). The interaction of UmuD with the β clamp seems to be important for facilitating a DNA damage checkpoint in *E. coli* (2,3), and the cleavage of UmuD to UmuD' may attenuate this checkpoint function (9). The UmuD-3A variant seems to bypass this switch, yet still binds the β clamp. In eukaryotes, covalent modification of PCNA with monoubiquitin or SUMO determines whether the cell utilizes DNA repair or potentially mutagenic translesion synthesis (16). Thus, access to sliding clamps is universally important for control and regulation of proteins acting at the replication fork.

REFERENCES

1. Friedberg, E. C., Walker, G. C., Siede, W., Wood, R. D., Schultz, R. A., and Ellenberger, T. (2005) *DNA Repair and Mutagenesis*, Second Ed., AMS Press, Washington, D.C.
2. Opperman, T., Murli, S., Smith, B. T., and Walker, G. C. (1999) *Proc. Natl. Acad. Sci. USA* **96**, 9218-9223
3. Sutton, M. D., and Walker, G. C. (2001) *J. Bacteriol.* **183**, 1215-1224
4. Ferentz, A. E., Walker, G. C., and Wagner, G. (2001) *EMBO J.* **20**, 4287-4298
5. Ferentz, A. E., Opperman, T., Walker, G. C., and Wagner, G. (1997) *Nat. Struct. Biol.* **4**, 979-983
6. Peat, T. S., Frank, E. G., McDonald, J. P., Levine, A. S., Woodgate, R., and Hendrickson, W. A. (1996) *Nature* **380**, 727-730
7. Sutton, M. D., Guzzo, A., Narumi, I., Costanzo, M., Altenbach, C., Ferentz, A. E., Hubbell, W. L., and Walker, G. C. (2002) *DNA Repair* **1**, 77-93
8. Sutton, M. D., Opperman, T., and Walker, G. C. (1999) *Proc. Natl. Acad. Sci. USA* **96**, 12373-12378
9. Sutton, M. D., Narumi, I., and Walker, G. C. (2002) *Proc. Natl. Acad. Sci. USA* **99**, 5307-5312

10. Becherel, O. J., Fuchs, R. P. P., and Wagner, J. (2002) *DNA Repair* **1**, 703-708
11. Beuning, P. J., Barsky, D., Sawicka, D., and Walker, G. C. *Mol. Microbiol.*, in press
12. Fujii, S., and Fuchs, R. P. (2004) *EMBO J.* **23**, 4342-4352
13. Indiani, C., McInerney, P., Georgescu, R., Goodman, M. F., and O'Donnell, M. (2005) *Mol. Cell* **19**, 805-815
14. Yang, J., Zhuang, Z., Roccasecca, R. M., Trakselis, M. A., and Benkovic, S. J. (2004) *Proc. Natl. Acad. Sci. USA* **101**, 8289-8294
15. Kannouche, P. L., Wing, J., and Lehmann, A. R. (2004) *Mol. Cell* **14**, 491-500
16. Gill, G. (2004) *Genes Dev.* **18**, 2046-2059
17. Vivona, J. B., and Kelman, Z. (2003) *FEBS Lett.* **546**, 167-172
18. Warbrick, E. (2000) *Bioessays* **22**, 997-1006
19. Duzen, J. M., Walker, G. C., and Sutton, M. D. (2004) *DNA Repair* **3**, 301-312
20. Dalrymple, B. P., Kongsuwan, K., Wijffels, G., Dixon, N. E., and Jennings, P. A. (2001) *Proc. Natl. Acad. Sci. USA* **98**, 11627-11632
21. Zemla, A. (2003) *Nucleic Acids Research* **31**, 3370-3374
22. Zemla, A., C., E. Z., Slezak, T., Kuczmarski, T., Rama, D., Torres, C., Sawicka, D., and Barsky, D. (2005) *Nucleic Acids Research* **33 (Web Server issue)**, W111-W115
23. Peat, T. S., Frank, E. G., McDonald, J. P., Levine, A. S., Woodgate, R., and Hendrickson, W. A. (1996) *Structure* **4**, 1401-1412
24. Luo, Y., Pfuetzner, R. A., Mosimann, S., Paetzel, M., Frey, E. A., Cherney, M., Kim, B., Little, J. W., and Strynadka, N. C. J. (2001) *Cell* **106**, 585-594
25. Bower, M., Cohen, F. E., and Dunbrack, J. R. L. (1997) *J. Mol. Biol.* **267**, 1268-1282
26. Beuning, P. J., Godoy, V. G., Simon, S. M., Jarosz, D. F., and Walker, G. C. *Methods Enzymol.*, in press
27. Turner, J., Hingorani, M. M., Kelman, Z., and O'Donnell, M. (1999) *EMBO J.* **18**, 771-783
28. Guzzo, A., Lee, M. H., Oda, K., and Walker, G. C. (1996) *J. Bacteriol.* **178**, 7295-7303
29. Lee, M. H., Guzzo, A., and Walker, G. C. (1996) *J. Bacteriol.* **178**, 7304-7307
30. Kulaeva, O. I., Wootton, J. C., Levine, A. S., and Woodgate, R. (1995) *J. Bacteriol.* **177**, 2737-2743
31. Lee, M. H., Ohta, T., and Walker, G. C. (1994) *J. Bacteriol.* **176**, 4825-4837
32. Wright, S. K., and Viola, R. E. (1998) *Anal. Biochem.* **265**, 8-14
33. Battista, J. R., Ohta, T., Nohmi, T., Sun, W., and Walker, G. C. (1990) *Proc. Natl. Acad. Sci. USA* **87**, 7190-7194
34. Nohmi, T., Battista, J. R., Dodson, L. A., and Walker, G. C. (1988) *Proc. Natl. Acad. Sci. USA* **85**, 1816-1820
35. Opperman, T., Murli, S., and Walker, G. C. (1996) *J. Bacteriol.* **178**, 4400-4411
36. Sutton, M. D., Farrow, M. F., Burton, B. M., and Walker, G. C. (2001) *J. Bacteriol.* **183**, 2897-2909
37. Harris, D. A. (1996) *Light Spectroscopy*, BIOS Scientific Publishers, Ltd. , Oxford, UK
38. Dohrmann, P. R., and McHenry, C. S. (2005) *J. Mol. Biol.* **350**, 228-239
39. Wagner, J., Fujii, S., Gruz, P., Nohmi, T., and Fuchs, R. P. (2000) *EMBO Reports* **1**, 484-488
40. McDonald, J. P., Frank, E. G., Levine, A. S., and Woodgate, R. (1998) *Proc Natl Acad Sci U S A* **95**, 1478-1483

41. Kazmirski, S. L., Zhao, Y., Bowman, G. D., O'Donnell, M., and Kuriyan, J. (2005) *Proc. Natl. Acad. Sci. USA* **102**, 13801-13806
42. Kong, X.-P., Onrust, R., O'Donnell, M., and Kuriyan, J. (1992) *Cell* **69**, 425-437
43. Bunting, K. A., Roe, S. M., and Pearl, L. H. (2003) *EMBO J.* **22**, 5883-5892
44. Jeruzalmi, D., Yurieva, O., Zhao, Y., Young, M., Stewart, J., Hingorani, M., O'Donnell, M., and Kuriyan, J. (2001) *Cell* **106**, 417-428
45. Wijffels, G., Dalrymple, B. P., Prosselkov, P., Kongsuwan, K., Epa, V. C., Lilley, P. E., Jergic, S., Buchardt, J., Brown, S. E., Alewood, P. F., Jennings, P. A., and Dixon, N. E. (2004) *Biochemistry* **43**, 5661-5671
46. Sommer, S., Boudsocq, F., Devoret, R., and Bailone, A. (1998) *Mol. Microbiol.* **28**, 281-291
47. Churchward, G., Belin, D., and Nagamine, Y. (1984) *Gene* **31**, 165-171
48. Oh Johanson, K., Haynes, T. E., and McHenry, C. S. (1986) *J. Biol. Chem.* **261**, 11460-11465
49. Humphrey, W., Dalke, A., and Schulten, K. (1996) *J. Molec. Graphics* **14**, 33-38

FOOTNOTES

We thank Prof. Robert Sauer (MIT) and his laboratory for use of the fluorimeter and for technical advice. We also thank Prof. Charles McHenry (Univ. of Colorado) for pSJS9 and helpful discussions. We thank Prof. Mike O'Donnell (Rockefeller Univ.) for the plasmid expressing His-HMK-β, Daniel Jarosz for assistance in preparing Fig. 7, and Michael Simon for careful reading of the manuscript. This work was supported by grant number CA21615 from the National Cancer Institute and NIEHS Center Grant Number P30ES02109 from the MIT Center for Environmental Health Sciences to G.C.W. and a postdoctoral fellowship from the Damon Runyon Cancer Research Foundation to P.J.B. S.M.S. was supported by a Cleo and Paul Schimmel Fellowship. Some of this work was performed under the auspices of the U.S. Department of Energy by the University of California, Lawrence Livermore National Laboratory under Contract W-7405-Eng-48.

Table 1. Strains and Plasmids

Strain	**Relevant Genotype**	**Reference**
AB1157	*argE3*	Laboratory stock
GW8017	AB1157 Δ*umuDC*	(28)
Plasmid		**Reference**
pGY9738	o_1^C *umuD'C;* pSC101-derived	(46)
pGY9739	o_1^C *umuDC;* pSC101-derived	(46)
pGB2	Vector; pSC101-derived	(47)
pSJS9	Ts λ repression, Kan^R	(48)

Table 2. Loss of Synthetic Lethality due to Mutations in UmuD b-binding motif

AB1157 pSJS9	**cfu (37 °C, per mg DNA per mL)**
pGY9738 (WT)	0
pGB2	4170
pGY9739-UmuD-3A	5600

FIGURE LEGENDS

Figure 1. **Homology model of the $UmuD_2$ dimer (trans, arms down).** Also see Fig. S1. One monomer is in blue, the other is in red. The residues mutated in UmuD-3A [T14 (orange); L17 F18 (purple)] are shown in space-filling rendering. The single Cys residue, Cys24, is shown in yellow. Ser60 is shown in green.

Figure 2. **The β-binding motif variants do not eliminate UV-induced mutagenesis.** *A* The putative β-binding motif in UmuD, with the variants indicated. *B* Induced mutation frequency of the indicated UmuD mutations in pGY9739 *umuDC* plasmids in GW8017 (Δ*umuDC*).

Figure 3. **UmuD variants are defective in cleavage.** *A* Immunoblot showing the stable production of UmuD variant proteins. *B* Immunoblot showing *in vivo* cleavage of UmuD variant proteins. Time points for each sample are 0 (before UV-irradiation) and 1, 2, and 3 h after UV irradiation. *C* UmuD cleavage *in vitro*. The (+) sign indicates the presence of the RecA/ssDNA nucleoprotein filament. The last two lanes show alkaline cleavage of UmuD.

Figure 4. **UmuD variants result in loss of the cold-sensitive phenotype.** The ratio of colony-forming units (cfu) of AB1157 per μg of transformed plasmid DNA when grown at 42 °C versus 30 °C is plotted for each UmuD construct.

Figure 5. **UV survival of UmuD variants.** Assays were performed with pGY9739 plasmids and derivatives in GW8017 (Δ*umuDC*): pGY9738 (*umuD'C*, ?); pGY9739-F18A (*umuDC* F18A, ?); pGY9739-D3A S60A (*umuDC* D3A S60A, +); pGY9739-F18A S60A (*umuDC* F18A S60A, -); pGY9739-D3A (*umuDC* D3A, ∗); pGY9739 (*umuDC*, ¦); pGB2 (empty vector, ?); pGY9739-S60A (*umuDC* S60A, ×).

Figure 6. **UmuD-3A arms are more easily cross-linked with BMH and more accessible to chemical modification than wild-type.** *A* Cross-linking the UmuD arms with BMH. Each UmuD variant that was cross-linked is indicated under the lanes. The time points were 0, 15, and 30 min after addition of BMH. The first lane shows molecular weight standards, with weights indicated in kDa. *B* DTNB titration of free thiol in UmuD. The complete reaction without protein was used as a blank, protein was added and absorbance was recorded at 412 nm for 15 min. $UmuD_2$ (¦) and $UmuD\text{-}3A_2$ (?) were present at 10 μM with 20 μM DTNB.

Figure 7. **UmuD binding as observed by tryptophan fluorescence.** *A* UmuD (filled circles) and UmuD-3A (open circles) bind with similar affinity yet cause opposite shifts in the Trp fluorescence emisson wavelength. The K_d of $UmuD_2$ is 5.5 ± 0.8 μM, while for that of $UmuD\text{-}3A_2$ is 6.1 ± 0.5 μM. *B* Structure of the β clamp (entry 2POL from the Protein Data Bank) showing the known sites of interaction of UmuD based on cross-linking experiments (red) (19) versus the site of interaction of the canonical β-binding motif (green) and the second site of interaction observed in the co-crystal structure with DinB (green, labeled "second site") (43,44). The single tryptophan, W122, is also indicated in yellow. Arrows indicate the dimer interface. The domains are labeled, I, II, and III. This image was prepared with VMD (49).

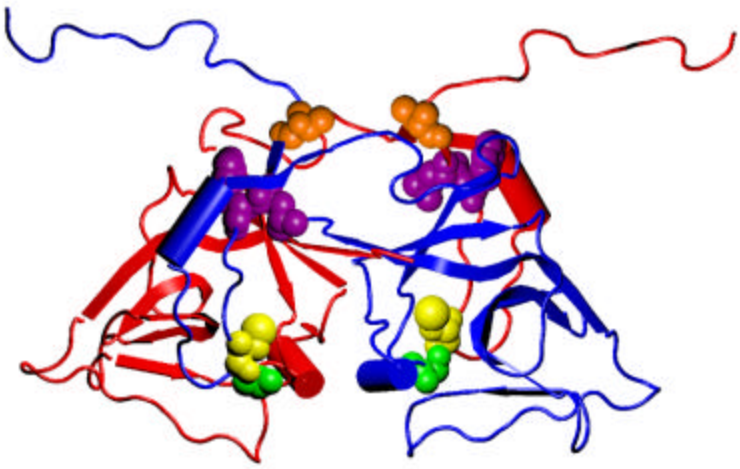

Figure 1.

A

UmuD

UmuD ^{14}TLDLF^{18}
UmuD-3A **A**LD**AA**

B

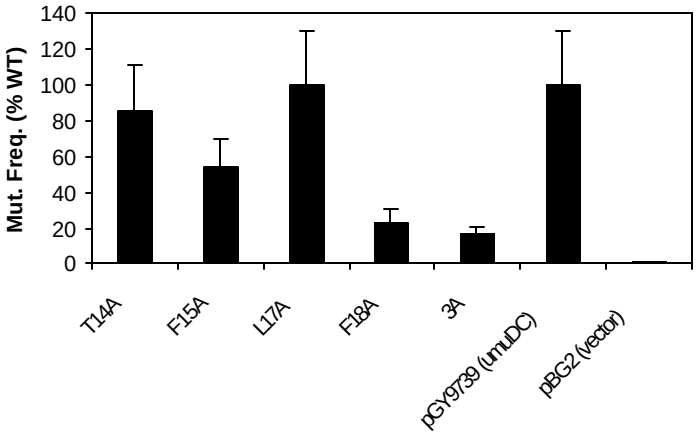

Figure 2.

A

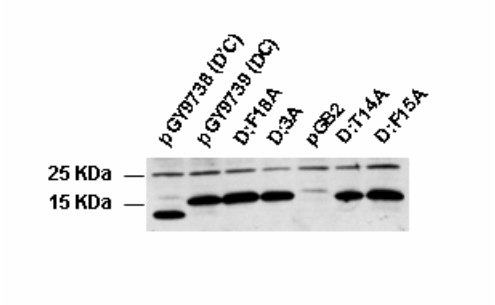
pGYB738 (D'C)
pGYB739 (DC)
D:F18A
D:3A
pGB2
D:T14A
D:F15A
25 KDa
15 KDa

B

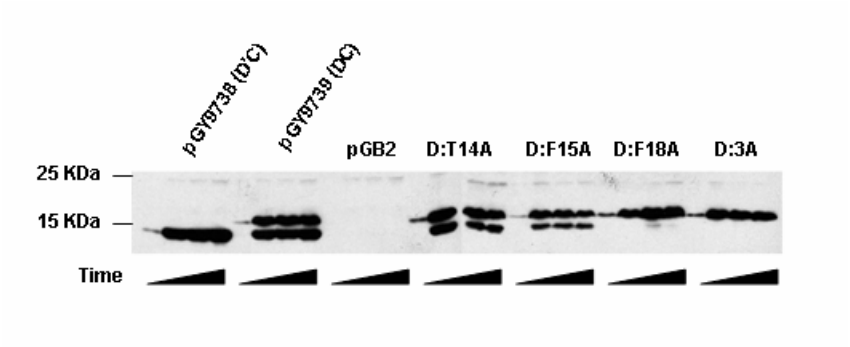
pGYB738 (D'C)
pGYB739 (DC)
pGB2
D:T14A
D:F15A
D:F18A
D:3A
25 KDa
15 KDa
Time

C

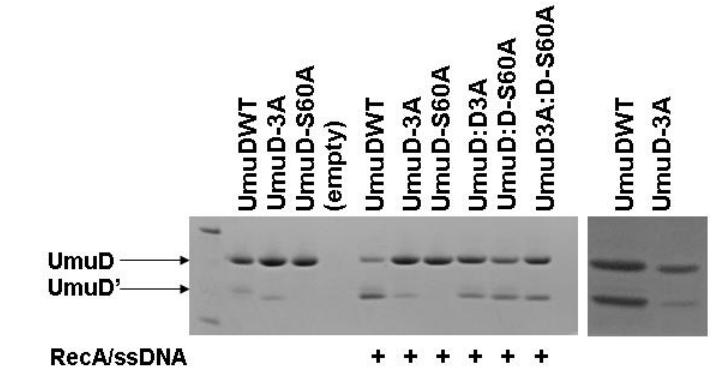
UmuDWT
UmuD-3A
UmuD-S60A
(empty)
UmuDWT
UmuD-3A
UmuD-S60A
UmuD:D3A
UmuD:D-S60A
UmuD3A:D-S60A
UmuDWT
UmuD-3A
UmuD
UmuD'
RecA/ssDNA
+ + + + + +

Figure 3.

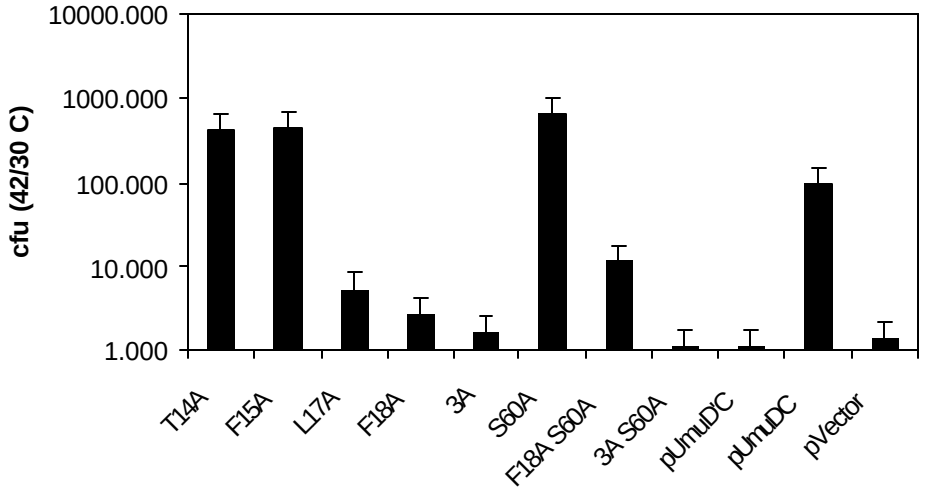
10000.000
1000.000
100.000
10.000
1.000
cfu (42/30 C)
T14A
F15A
L17A
F18A
3A
S60A
F18A S60A
3A S60A
pUmuDC
pUmuDC
pVector

Figure 4.

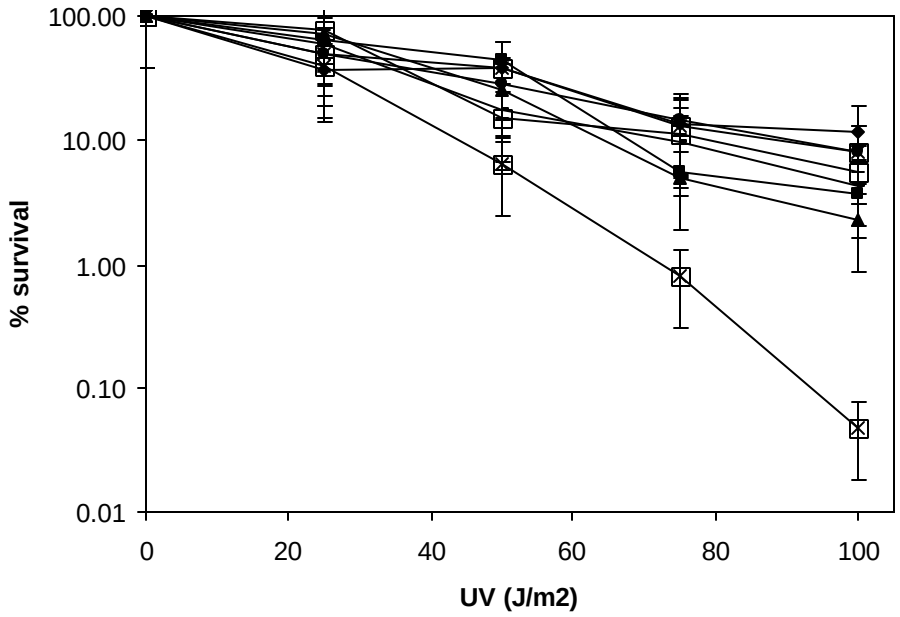

Figure 5.

A

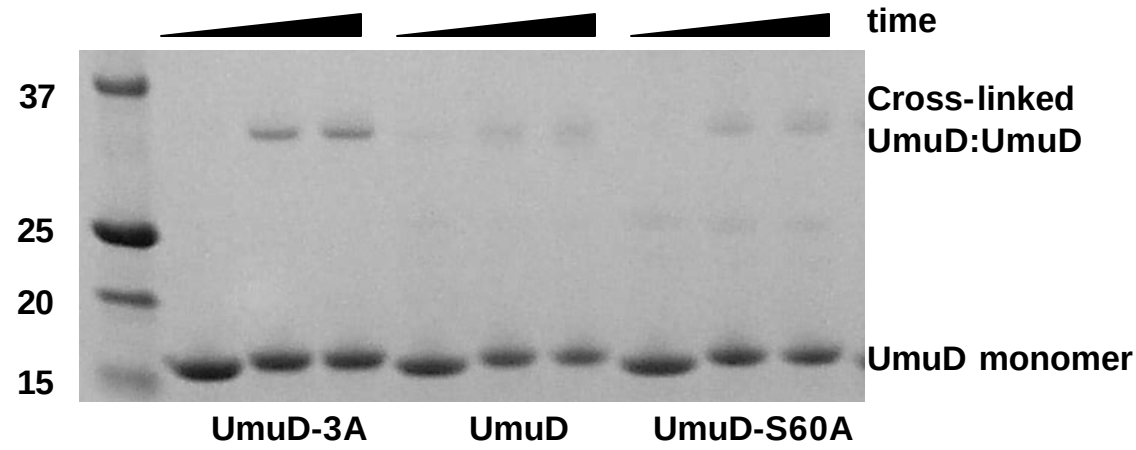
time
37
25
20
15
Cross-linked
UmuD:UmuD
UmuD monomer
UmuD-3A
UmuD
UmuD-S60A

B

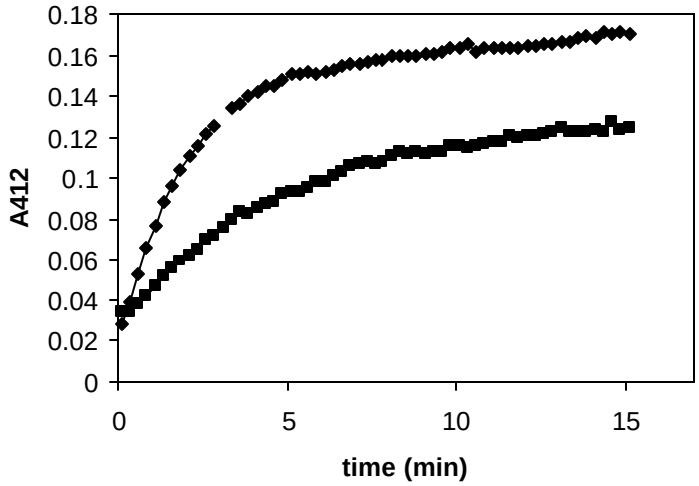
0.18
0.16
0.14
0.12
0.1
0.08
0.06
0.04
0.02
0
A412
0
5
10
15
time (min)

Figure 6.

A

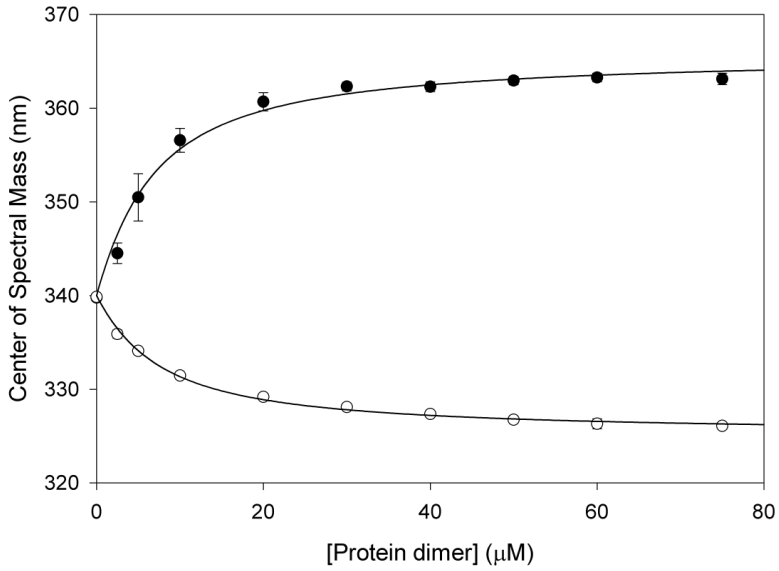
370
360
350
340
330
320
Center of Spectral Mass (nm)
0
20
40
60
80
[Protein dimer] (μM)

B

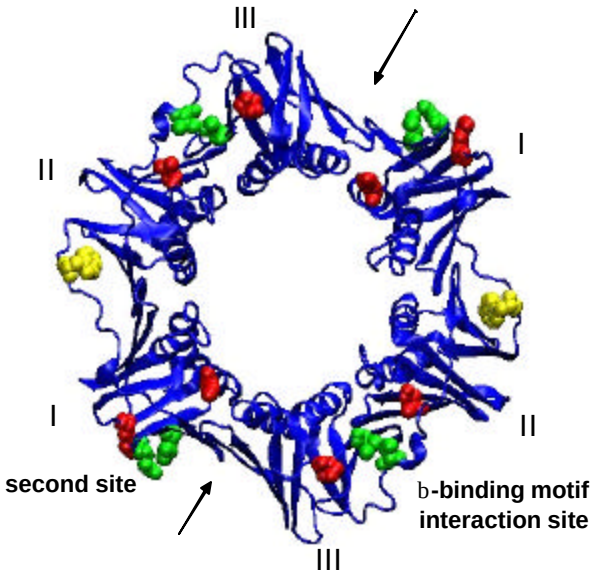
III
I
II
I
II
second site
b-binding motif
interaction site
III

Figure 7.